A high-temperature shock-tube study on the optical properties and pyrolysis of anisole

S. Zabeti*, M. Aghsaee, M. Fikri, O. Welz, C. Schulz*

Institute for Combustion and Gas Dynamics – Reactive Fluids, University of Duisburg-Essen, Duisburg, Germany

Abstract

Temporally and spectrally resolved ultraviolet (UV) absorption and spectrally resolved laser induced fluorescence (LIF) of anisole have been studied at temperatures between 565 and 1560 K and pressures of 1.3 and 2.9 bar behind reflected shock waves. UV absorption spectra of anisole were acquired in the spectral range 240–310 nm. LIF spectra of anisole were recorded at fixed reaction times behind the reflected shock using 266-nm laser excitation. To aid interpretation of these experiments, pyrolysis of anisole was investigated using a shock tube coupled to high-repetition-rate time-of-flight mass spectrometry (HRR-TOF-MS) for time-resolved multispecies measurements.

Introduction

Laser-induced fluorescence (LIF) of organic tracer molecules is a powerful non-intrusive imaging technique to investigate fuel concentration, equivalence ratio, and temperature in combustion applications [1]. Various types of organic species, such as ketones and aromatic compounds have become popular as fluorescent tracers over the past two decades. To obtain reliable results from tracer-LIF measurements, the photophysical and chemical kinetics properties of the tracers have to be known. So far, most of the studies have focused on the photophysical properties of tracers [1]. In high-temperature applications, however, the tracer might decompose on the time scale of the measurements. Furthermore, the decomposition behavior of the tracer might be different to the behavior of the parent fuel [2]. As a consequence, decomposition of the tracer or interfering signals originating from decomposition products can hinder the applicability of this technique [3-5]. Therefore, in addition to the photophysical properties of tracers, their decomposition kinetics and the photophysical properties of their decomposition products need to be taken into account.

Shock tubes have already been successfully applied to determine ultraviolet (UV) absorption and LIF spectra and kinetics of tracers under engine-relevant conditions [5, 6]. Compared to widely used static and flow cells, in which the long residence time of the gas mixture prevents high-temperature measurements, shock tubes enable studying the photophysical and kinetics of tracers at high temperature and on short time scales (less than a millisecond).

Anisole was recently suggested as a fluorescence tracer due to its favorable optical properties [7-9], and several studies were performed, which investigated the photophysics of anisole and which applied anisole as tracer in combustion environments. Hirasawa et al. [10] performed LIF measurements of seven fluorescent species including anisole to propose the best pair of fluorescent species for two-dimensional gas temperature profiles based on two-color LIF. Pasquier et al. [11] chose anisole as a fluorescence tracer due to the strong fluorescence quenching by O_2 to investigate the equivalence ratio field of a propane/air flame. Tran et al. [9] investigated the influence of temperature, pressure, and different ambient gases on the fluorescence spectrum and the relative fluorescence quantum yield of anisole in a high temperature cell. Additionally, they reported the UV absorption spectrum of anisole in a bath of CO_2 between 473 and 823 K at 1 bar. Faust et al. [7] recently studied the fluorescence spectra, lifetimes and relative fluorescence quantum yield of anisole as a function of temperature, pressure, and O_2 partial pressure after 266-nm laser excitation in a heated flow cell up to 977 K. More recently, Faust et al. [8] compared relative fluorescence signal intensities of anisole and three common fluorescence tracers (toluene, naphthalene, and acetone) in a jet fluid seeded with tracer upon 266-nm excitation. Here anisole yielded the highest total fluorescence signal among those tracers in both N_2 and air.

Several studies investigated the kinetics and mechanism of anisole decomposition [12-16]. Thermal decomposition of anisole occurs through dissociation of the C-O bond in the methoxy group forming CH_3 and the resonance stabilized phenoxy (C_6H_5O) radical:

$$C_6H_5OCH_3 \rightarrow C_6H_5O + CH_3. \qquad (1)$$

The phenoxy radical can undergo subsequent bimolecular reactions with species such as H-atoms to produce phenol or with CH_3 to produce cresol isomers, or it can unimolecularly decompose to cyclopentadienyl (C_5H_5) + CO. Cyclopentadienyl has been suggested as a main precursor of naphthalene and heavier polycyclic aromatic hydrocarbons [14].

In the present work, we report temporally and spectrally resolved UV absorption measurements during anisole pyrolysis at high temperature behind reflected shock waves. Additionally, fluorescence spectra of anisole and its pyrolysis products are measured at different temperatures using 266-nm laser excitation at selected reaction times. To improve our understanding about the stability and pyrolysis kinetics of anisole, we additionally present time-resolved multiple species measurements using high-repetition-rate time-of-flight

* Corresponding authors: siavash.zabeti@uni-due.de, christof.schulz@uni-due.de

mass spectrometry (HRR-TOF-MS) behind reflected shock waves.

Experiment

The setup used for the UV absorption and LIF measurements has been described in detail in Ref. [5] and the one for the HRR-TOF-MS experiments in Ref. [17]. Here, we only give a brief overview.

The optical and HRR-TOF-MS experiments were performed in two different stainless steel shock tubes with an inner diameter of 80 mm. The incident shock velocity was measured using four piezoelectric pressure transducers placed near the end wall of the tube. Temperature and pressure behind the reflected shock were calculated from the velocity of the incident shock wave and the initial conditions in the driven section based on ideal one-dimensional shock equations using the CHEMKIN-II package [18].

UV absorption spectra of anisole were recorded temporally and spectrally resolved using a deuterium lamp (30 W, Heraeus D200 F-HV) as a continuous broadband UV light source. The collimated light passed through quartz windows (8 mm diameter) of the shock tube located 1 cm upstream of the end flange and was focused on the entrance slit of a spectrograph (Acton SP 2300i, Princeton instruments, 150 g/mm grating) coupled to a UV-sensitive back-illuminated EMCCD camera (Ixon, Andor), which was used in kinetic mode. With the arrival of the incident shock wave at the pressure transducers, a delay generator (DG535, Stanford Research systems) was triggered, which started the data acquisition. The temporal resolution of the detection setup was ~50 µs.

UV absorption spectra were investigated as a function of reaction time by time-resolved monitoring the intensity of absorbed radiation $I(\lambda,t)$ relative to the incident radiation $I_0(\lambda)$. At temperatures where anisole is stable on the experimental time scale, the absorption cross-section $\sigma(\lambda)$ of anisole was calculated using the Beer–Lambert's law,

$$\sigma(\lambda) = -\frac{\ln(I(\lambda)/I_0(\lambda))}{cl}, \qquad (2)$$

with the incident and transmitted light intensities $I_0(\lambda)$ and $I(\lambda)$, respectively, the path length (inner diameter of shock tube) l and the concentration of anisole behind the reflected shock c. At temperatures where pyrolysis of anisole cannot be neglected, we derived an effective absorption cross-section $\sigma_{\text{eff}}(\lambda, t)$ that is based on the initial concentration of anisole behind the reflected shock c_0 [5]:

$$\sigma_{\text{eff}}(\lambda, t) = -\frac{\ln(I(\lambda,t)/I_0(\lambda))}{c_0 l}. \qquad (3)$$

For the measurements of spectrally resolved LIF, the test gas was excited behind the reflected shock at selected reaction times using a pulsed frequency-quadrupled Nd:YAG laser at 266 nm. The laser beam was introduced through an optical port in the sidewall of the shock tube 30 mm away from the end flange. The emitted fluorescence light was collected perpendicular to the laser beam through a quartz window in the end flange and focused on the entrance slit of a spectrograph (Acton SP 2150i, Princeton instruments, 150 g/mm grating) coupled to an intensified CCD camera (Imager Intense, LaVision). A delay generator (DG535, Stanford Research Systems) synchronized the laser and camera using the signal of a pressure transducer as trigger input. The fluorescence signal was obtained from single shot data by integrating the measured spectrum along the spatial axis of the two dimensional array that was recorded using the spectrograph and ICCD to improve the signal-to-noise ratio. A low-pressure mercury discharge lamp was used to calibrate the wavelength scale of the spectrograph. The wavelength-dependent sensitivity of the detection system was corrected using measurements of the emission spectra of a deuterium (for $\lambda < 400$ nm) and a tungsten lamp (for $\lambda > 350$ nm) with known spectral radiance. Background signals were taken before the experiments and subtracted from the measured images.

In the HRR-TOF-MS experiments, multispecies time profiles during anisole pyrolysis were measured in intervals of 10 µs. The mass spectrometer is coupled to the shock tube through a conical nozzle with a diameter of 60 µm placed at the center of the end flange. The mass spectrometer is equipped with an electron impact ion source with two-stage ion extraction and a microchannel plate (MCP) detector and can be operated in either linear or reflectron mode. The kinetic energy of the ionizing electrons can be varied between 5 and 85 eV. Here we used an energy of 45 eV.

Gas mixtures for both optical and HRR-TOF-MS experiments were prepared in mixing vessels (50 l) and allowed to homogenize before use. The HRR-TOF-MS measurements were done with mixtures of 0.5% anisole and 0.5% Ar as an internal standard [17, 19] with Ne as the bath gas. The optical experiments employed mixtures of 0.25% or 0.5% anisole in a bath of argon. The experiments were performed in the absence of O_2 to prevent quenching of the fluorescence in the optical experiments and oxidation of anisole.

Results

HRR-TOF-MS experiments

HRR-TOF-MS experiments of anisole pyrolysis were performed between 930 and 1530 K at pressures ranging from 0.88 to 1.67 bar. These experiments simultaneously probe the temporal behavior of anisole and its decomposition products and therefore aid interpretation of the optical experiments with respect to the thermal stability of anisole and to products formed from anisole pyrolysis under comparable conditions.

Figure 1 shows time profiles of anisole as a function of temperature. At 930 K anisole is stable on the experimental time scale, but starts to decompose with increasing temperature. At 1050 K, about 20% of anisole decompose within the test time of 1.4 ms, and at 1530 K, anisole is completely decomposed during the first 200 µs. These observations are in qualitative agreement

with results from Lin and Lin [16], who measured the rate coefficient for anisole decomposition between 1000 and 1580 K and found lifetimes of anisole of 20 ms at 1000 K and 0.3 µs at 1500 K. These results show that decomposition of anisole can be neglected in the optical experiment up to ~950 K, but needs to be accounted for at higher temperature.

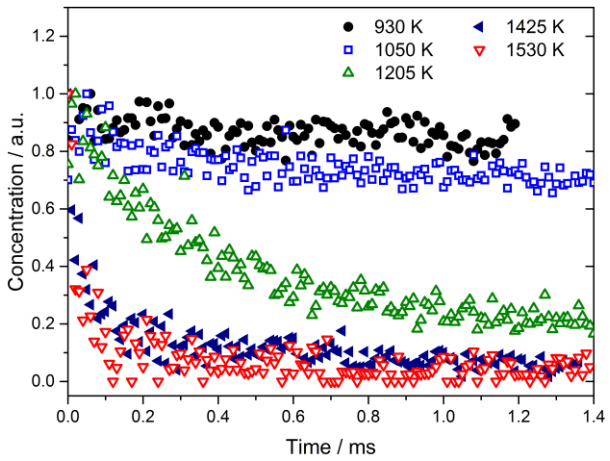

Fig. 1: Concentration-time profile during anisole pyrolysis as a function of temperature.

Figure 2 shows two product mass spectra from anisole pyrolysis, one for 930 K and 1.18 bar, where anisole is stable, and the other for 1425 and 1.6 bar, where most of the anisole initially present is already decomposed. From the mass spectrum at 930 K it becomes obvious that besides formation of the parent ion ($C_7H_8O^+$) of anisole at a mass-to-charge ratio (m/z) of 108, fragmentation of ionized anisole produces strong signal at the masses corresponding to $C_6H_5O^+$ (m/z = 93), $C_6H_6^+$ (m/z = 78), $C_5H_5^+$ (m/z = 65), $C_4H_3^+$ (m/z = 51), and $C_3H_3^+$ (m/z = 39). Strong signal at m/z = 20 and 40 corresponds to the bath gas Ne and the internal standard Ar, respectively.

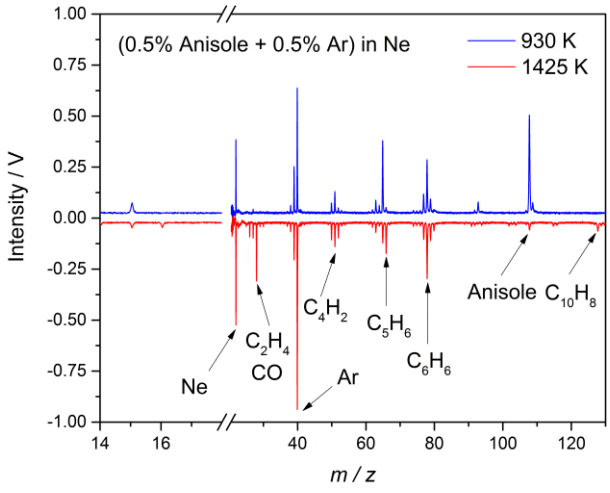

Fig. 2: Mass spectra of anisole pyrolysis integrated over reaction time between 1 and 1.5 ms. The mixtures consisted of 0.5% anisole and 0.5% Ar in Ne.

The weak signal at m/z = 108, the parent mass of anisole in the mass spectrum of the 1425 K experiment compared to the signal of the internal standard Ar immediately shows that most of the anisole is decomposed after 1 ms, suggesting that the other peaks observed (except m/z = 20 and 40, see above) correspond to products from pyrolysis of anisole. Although we have not calibrated the spectra of the pure compounds of potential pyrolysis products, which would enable deriving quantitative information from this data, comparison with mass spectra from the NIST database (taken with 70 eV electron impact ionization) [20] and with results from literature studies on anisole pyrolysis [15] allows drawing some qualitative conclusions. Scheer et al. [15] detected naphthalene ($C_{10}H_8$) and benzene (C_6H_6) as products from anisole pyrolysis. Signals at m/z = 128 ($C_{10}H_8$) and 78 (C_6H_6) in our mass spectra are consistent with formation of naphthalene and benzene, respectively. Whereas fragmentation of naphthalene following electron impact ionization at 70 eV is comparably minor [20], fragmentation of ionized C_6H_6 contributes to the observed product signal at m/z = 39, 50, 51, and 52. Signal at m/z = 66 (C_5H_6) observed in our product mass spectrum at 1425 K might suggest formation of cyclopentadiene. For further assignments of the observed peaks to products and for a quantification of product yields, calibration measurements with the pure compounds are necessary, which is reserved for future work.

UV absorption experiments

Temporally and spectrally resolved UV absorption of anisole diluted in argon was measured behind reflected shock waves. Measurements were performed over a wide temperature range between 565 and 1450 K at a pressure of 1.5 bar or 2.9 bar for a mixture of 0.25 or 0.5% anisole in argon. In addition, a room temperature UV absorption spectrum was taken prior to arrival of the shock wave in the test section at a pressure of ~120 mbar. At low temperature (T < 1000 K), where decomposition of anisole is not expected on the experimental time scale, absorption cross-sections were determined using Beer-Lambert's law (Eq. 2).

Figure 3 shows UV absorption cross-sections of anisole between 240 and 310 nm as a function of temperature. An absorption band centered at about 270 nm is observed for anisole resulting from a π–π* ($S_0 - S_1$) electronic transition. With increasing temperature, the maximum of the absorption band shifts towards longer wavelength and the spectrum broadens. At room temperature we found an absorption cross-section at the peak maximum of $\sigma_{270\,nm}(296\,K) = 4.2 \times 10^{-18}$ cm^2 and a full width at half maximum (FWHM) of ~19 nm. As is the case for toluene [21], the spectrum of anisole at room temperature has a fine structure which is no longer visible in the experiments at higher temperatures. Note that the absorption spectra (solid lines) in Fig. 3 were measured with a spectral resolution of ~7 nm, which does not enable to fully resolve the fine structure (cf. the absorption spectrum of anisole taken with a higher spectral resolution of 3 nm shown as the dashed line in Fig.

3, corresponding to $\sigma_{270\ nm}(296\ K) = 5.3 \times 10^{-18}\ cm^2$). Tran et al. [9] measured the absorption cross-section of anisole at room temperature in a bath of CO_2 and obtained values that are approximately a factor of three lower than our results. The reason for this substantial deviation is unclear. We note, however, that we observed evidence of adsorption of anisole on the surface of our shock tube. In the room-temperature absorption measurements, we therefore took care to passivate the walls before taking a measurement. In the measurements at higher temperature, the room-temperature absorption measured in the pre-shock region (i.e., before the shock wave arrived at the optical axis) provided an internal calibration of the anisole concentration, so that the higher-temperature measurements on the absorption cross-section of anisole are unaffected by adsorption.

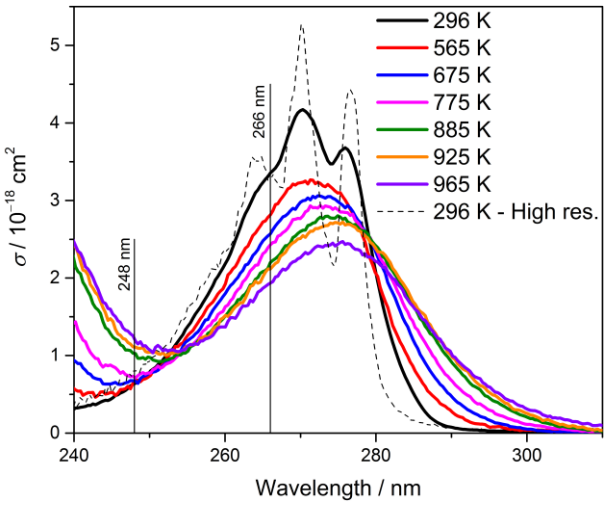

Fig. 3: Absorption cross-section of a 0.5% mixture of anisole in Ar at room temperature (120 mbar) and at higher temperatures (1.5 bar) with a spectral resolution of ~7 nm; Dashed line: room temperature spectrum with higher spectral resolution (~3 nm).

As observed in the HRR-TOF-MS experiments, decomposition of anisole becomes relevant under our conditions at T > ~1000 K, leading to new absorbing species with optical properties potentially different from anisole. Figure 4 shows the time behavior of the effective absorption cross-section (Eq. 3) around 266 nm as a function of temperature. If anisole is stable on the experimental time scale, the effective absorption cross-section equals the absorption cross-section of pure anisole. In this case, we would expect a plateau in the time behavior of σ_{eff} after the arrival of the reflected shock wave at $t = 0$. This behavior approximately occurs in the experiment at 1040 K, where $\sigma_{eff,\ 266\ nm}$ at $t > 0$ is close to the value of $\sigma_{266\ nm}(965\ K)$ (cf. Fig. 3). Note that the early time-rise present in the traces shown in Fig. 3 is due to the limited time resolution (~50 µs) of the experiment.

At higher temperature, $\sigma_{eff,\ 266\ nm}$ strongly increases with temperature, which can be rationalized by formation of products from anisole decomposition, which absorb stronger than anisole at 266 nm. This effect can be seen best in the time profile taken at 1190 K (blue line in Fig. 4), where a slow increase in $\sigma_{eff,\ 266\ nm}$ occurs for ~400 µs after passage of the reflected shock wave. The increase in signal and hence the rate of formation of pyrolysis products becomes larger with increasing temperature. In addition, a second region with a further increase in $\sigma_{eff,\ 266\ nm}$ after ~600 µs occurs in the experiment at 1450 K, suggesting formation of secondary species during the pyrolysis process. Modeling of the observed effective absorption cross-sections at these temperatures require knowledge of the high-temperature absorption cross-sections of pyrolysis products of anisole and a chemical kinetics model that would predict the time behavior of the pyrolysis system. To the best of our knowledge, high-temperature absorption products are unknown for the likely main products cyclopentadiene and naphthalene. The small absorption cross-section of benzene of $2 \times 10^{-20}\ cm^2$ at 266 nm [22] suggests that benzene is not responsible for the observed increase in $\sigma_{eff,\ 266\ nm}$ at higher temperature.

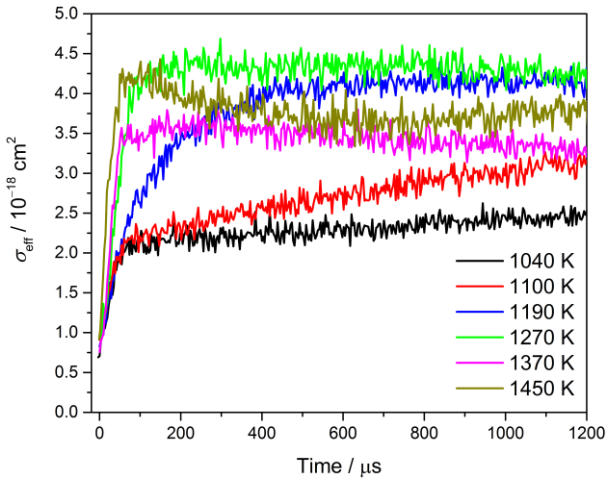

Fig. 4: Effective absorption cross-section σ_{eff} (Eq. (3)) at 266 nm of a mixture containing 0.25% anisole in argon for various temperatures at a pressure of 2.9 bar as a function of reaction time. Time zero marks the arrival of the reflected shock wave at the detection window.

LIF measurements

To investigate the fluorescence behavior of anisole at high temperatures, the LIF emission spectrum was measured at a reaction time of 160 µs following 266-nm laser excitation. Figure 5 shows the measured spectra at 296 and 940 K. The absolute fluorescence intensity decreases by ~2 orders of magnitude between 296 and 940 K. Because the absorption cross-section of anisole at 266 nm only decreases by about a factor of two over this temperature range (cf. Fig. 3), this strong decrease in the fluorescence intensity is mostly due to the decrease of the fluorescence quantum yield as a function of temperature. This assignment is qualitatively consistent with results from Faust et al., who report a drop in the fluorescence quantum yield of anisole following 266-nm excitation by a factor of ~300 between 300 and ~880 K [7]. The LIF emission spectrum of anisole at

room temperature occurs in the 270–360-nm wavelength range with a peak at around 290 nm. With increasing temperature, the LIF spectrum of anisole shifts to the red and the width of the feature also increases. To better visualize the red shift in the emission spectrum, the spectra presented in Fig. 5 are normalized to their respective peak maxima. Faust et al. [7] reported a red shift in the peak maximum of the LIF emission spectrum of anisole of ~3 nm per 100 K in a bath of nitrogen, whereas Tran et al. [9] reported a red-shift of 2.5 nm per 100 K in a bath of CO_2. Our measurements taken at 296 and 940 K in a bath of Ar suggest a red shift of ~2.2 nm per 100 K.

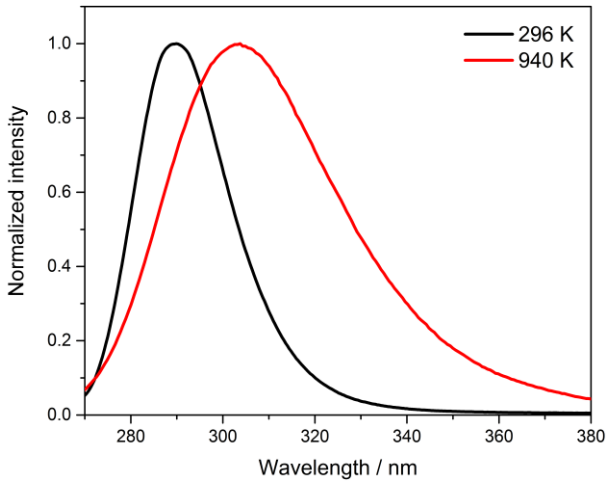

Fig. 5: Normalized LIF emission spectra of anisole at 296 and 940 K at a pressure of 1.5 bar after excitation at 266 nm and at 160 µs after the arrival of the reflected shock wave.

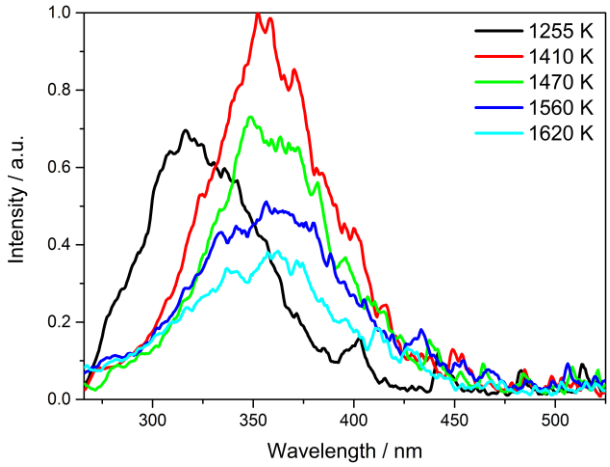

Fig. 6. LIF emission spectra during pyrolysis of anisole as a function of temperature at 1.3 bar after excitation at 266 nm and at 260 µs after the arrival of the reflected shock wave.

We performed additional LIF experiments between 1250 and 1620 K at a reaction time of 260 µs, where pyrolysis of anisole is significant (cf. Fig. 1). As shown in Figure 6, the spectra at higher temperature differ significantly from the ones at lower temperatures with the appearance of new spectral features far red-shifted compared to the original anisole spectrum. The LIF intensities shown in this figure are directly comparable to each other, showing that the trend observed at lower temperature of strongly decaying fluorescence intensity with temperature no longer persists at higher temperature. This result can qualitatively be explained by the formation of pyrolysis products with different fluorescence properties than anisole itself.

Conclusions

Spectrally and temporally resolved UV absorption of anisole was studied over a wide temperature range (565 – 1450 K) behind reflected shock waves. From measurements up to 965 K, where anisole is stable on the experimental time scale, we determined the absorption cross-section of anisole between 240 and 310 nm. We observed a broadening and red shift of the absorption spectrum and a decrease of the absorption cross-section at 266 nm with increasing temperature.

The temporal behavior of the absorption was investigated as a function of temperature with a time resolution of 50 µs. Here, interpretation of the results was supported by HRR-TOF-MS experiments coupled to a shock tube, which probes the reacting mixture with a time resolution of 10 µs and can monitor multiple species simultaneously. These experiments showed that under our conditions, anisole is stable up to ~950 K on the experimental time scale of ~1.5 ms and starts to decompose as the temperature is further increased. Results from the HRR-TOF-MS experiments are consistent with formation of naphthalene, benzene, and cyclopentadiene from anisole pyrolysis. In the UV-experiments, we observed an increase in the absorption signal at temperatures where anisole decomposes, suggesting that the decomposition products are stronger absorbers than anisole itself.

In addition, we measured LIF spectra between 296 and 1560 K behind the reflected shock using 266-nm excitation. Below 1000 K, where anisole is stable on the experimental time scale, the signal intensity of anisole-LIF decreases dramatically with increasing temperature mostly due to the decrease of the fluorescence quantum yield. Above 1400 K, the LIF spectrum shows a more significant red shift and discontinuity in the strong signal decrease found at lower temperature, suggesting contributions from decomposition products of anisole.

Acknowledgments

The authors gratefully acknowledge financial support by the German Research Foundation (SCHU 1369/9-2) and thank Birgit Nelius and Ludger Jerig (University of Duisburg-Essen) for technical support.

References

[1] C. Schulz, V. Sick, Prog. Energy Combust Sci. 31 (2005) 75-121.
[2] V. Sick, C. K. Westbrook, Proc. Combust. Inst. 32 (2009) 913–920.

[3] N. Graf, J. Gronki, C. Schulz, T. Baritaud, J. Cherel, P. Duret, J. Lavy, SAE Technical Paper Series 2001-01-1924 (2001).
[4] C. Schulz, J. Gronki, S. Andersson, SAE Technical Paper Series 2004-01-1917 (2004).
[5] S. Zabeti, A. Drakon, S. Faust, T. Dreier, O. Welz, M. Fikri, C. Schulz, Appl. Phys. B (2014) 1-13.
[6] J. D. Koch, J. Gronki, R. K. Hanson, J. Quant. Spectr. Rad. Trans. 109 (2008) 2037-2044.
[7] S. Faust, T. Dreier, C. Schulz, Appl. Phys. B 112 (2013) 203-213.
[8] S. Faust, M. Goschütz, S. Kaiser, T. Dreier, C. Schulz, Appl. Phys. B 117 (2014) 183-194.
[9] K. H. Tran, C. Morin, M. Kühni, P. Guibert, Appl. Phys. B 115 (2014) 461-470.
[10] T. Hirasawa, T. Kaneba, Y. Kamata, K. Muraoka, Y. Nakamura, J. Vis. 10 (2007) 197-206.
[11] N. Pasquier, B. Lecordier, M. Trinité, A. Cessou, Proc. Combust. Inst. 31 (2007) 1567-1574.
[12] A. V. Friderichsen, E.-J. Shin, R. J. Evans, M. R. Nimlos, D. C. Dayton, G. B. Ellison, Fuel 80 (2001) 1747-1755.
[13] E. B. Hemings, G. Bozzano, M. Dente, E. Ranzi, Chem. Eng. Trans. 24 (2011) 61-66.
[14] M. Nowakowska, O. Herbinet, A. Dufour, P.-A. Glaude, Combust. Flame 161 (2014) 1474-1488.
[15] A. M. Scheer, C. Mukarakate, D. J. Robichaud, G. B. Ellison, M. R. Nimlos, J. Phys. Chem. A 114 (2010) 9043-9056.
[16] C. Y. Lin, M. C. Lin, J. Phys. Chem. 90 (1986) 425-431.
[17] S. Dürrstein, M. Aghsaee, L. Jerig, M. Fikri, C. Schulz, Rev. Sci. inst. 82 (2011) 084103.
[18] R. J. Kee, F. M. Rupley, J. A. Miller, M. E. Coltrin, J. F. Grcar, E. Meeks, H. K. Moffat, A. E. Lutz, G. Dixon-Lewis, M. D. Smooke, J. Warnatz, G. H. Evans, R. S. Larson, R. E. Mitchell, L. R. Petzold, W. C. Reynolds, M. Carcotsios, W. E. Stewart, P. Glarborg, C. Wang, O. Adigun, CHEMKIN Collection, Reaction Design, Inc, San Diego, CA, 2009.
[19] I. Krizancic, M. Haluk, S. H. Cho, O. Trass, Rev. Sci. Inst. 50 (1979) 909-915.
[20] P. J. Linstrom, W. G. Mallard (Eds.), NIST Chemistry WebBook, NIST Standard Reference Database Number 69, National Institute of Standards and Technology, Gaithersburg, MD, 2003.
[21] W. Koban, J. D. Koch, R. K. Hanson, C. Schulz, Phys. Chem. Chem. Phys. 6 (2004) 2940-2945.
[22] M. A. Oehlschlaeger, D. F. Davidson, R. K. Hanson, Proc. Combust. Inst. 31 (2007) 211–219.